Soils and Foundations 2012;52(3):539–549

The Japanese Geotechnical Society

Soils and Foundations

www.sciencedirect.com
journal homepage: www.elsevier.com/locate/sandf

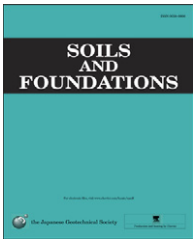

Experiments and predictions of physical properties of sand cemented by enzymatically-induced carbonate precipitation

Hideaki Yasuhara[a,*], Debendra Neupane[a], Kazuyuki Hayashi[b], Mitsu Okamura[a]

[a]*Department of Civil and Environmental Engineering, Ehime University, Matsuyama 790-8577, Japan*
[b]*Department of Civil Engineering, Wakayama National College of Technology, 77, Nadacho Noshima, Gobo 644-0023, Japan*

Available online 8 June 2012

Abstract

A grouting technique that utilizes precipitated calcium carbonate as a cementing material is presented. The enzyme urease is used to enhance the rate and the magnitude of the calcium carbonate precipitation. Evolutions in the mechanical and the hydraulic properties of treated sand samples are examined through unconfined compression and permeability tests, respectively. The grout is mainly composed of urease, which bio-catalyzes the hydrolysis of urea into carbon dioxide and ammonia, urea, and calcium chloride solutions. This method employs chemical reactions catalyzed by the enzyme, and ultimately acquires precipitated calcium carbonate within soils. The mechanical test results show that even a small percentage of calcium carbonate, precipitated within soils of interest, brings about a drastic improvement in the strength of the soils compared to that of untreated soils—the unconfined compressive strength of the samples treated with <10 vol% calcium carbonate precipitation against the initial pore volume ranges from $\sim$400 kPa to 1.6 MPa. Likewise, the hydraulic test results indicate the significant impervious effects of the grouting technique—the permeability of the improved samples shows more than one order of magnitude smaller than that of the untreated soils. Evolutions in the measured hydraulic conductivity and porosity are followed by a flow simulator that accounts for the solute transport process of the injected solutions and the chemical reaction of the calcite precipitation. Predictions of the changes in permeability with time overestimate the test measurements, but those of the changes in porosity show a good agreement with the actual measurements, indicating that such simulations should become a significant supplementary tool when considering real site applications.

Keywords: Grouting; Chemical; Compressive strength; Permeability; Laboratory test

1. Introduction

Chemical grouting has been used occasionally as a countermeasure against the liquefaction of the ground beneath existing structures. Recently, a novel grouting method that utilizes precipitated calcium carbonate as a cementing material has been examined. The precipitation of calcium carbonate is induced by the microbial metabolism (e.g., Stocks-Fischer et al., 1999; Nemati et al., 2005; DeJong et al., 2006). This technology, using the microbial metabolism, may be effective for stiffening soils of interest and for reducing the permeability of the soils. However, the evolutions in the mechanical and the hydraulic properties induced by the microbial metabolism may not be straightforward enough to be controlled, because it may be impossible to constrain the extinction and/or the generation of living bacteria in natural environments.

The research on calcium carbonate precipitation by bacteria has been mainly conducted using ureolytic bacteria. These bacteria indirectly produce precipitated calcium carbonate by a urease enzyme. The bacterium selected

*Corresponding author. Tel./fax: +81 89 927 9853.
E-mail address: hide@cee.ehime-u.ac.jp (H. Yasuhara).
Peer review under responsibility of The Japanese Geotechnical Society.

ELSEVIER Production and hosting by Elsevier

0038-0806
http://dx.doi.org/10.1016/j.sandf.2012.05.011

for research on calcium carbonate precipitation, containing the urease enzyme, is typically *Sporosarcina pasteurii*. The microbial-induced carbonate precipitation (MICP) has been evaluated as a soil-strengthening process, concluding that MICP has the potential to improve the mechanical properties of porous materials on a typical sample scale (Le Metayer-Levrel et al., 1999; Nemati and Voordouw, 2003; DeJong et al., 2006; Whiffin et al., 2007; Sugimoto and Kuwano, 2008), and on a larger container scale (Van der Ruyt and van der Zon, 2009; van Paassen et al., 2010). In this MICP technique, the transport and the fixation of the bacteria of interest are significant issues for achieving a suitable level of improvement of the saturated porous media, and thus, have been studied to this end (Murphy and Ginn, 2000; Foppen and Schijven, 2006; Whiffin et al., 2007; Harkes et al., 2010). In contradiction to the rigorous experimental works on this topic, the theoretical and/or numerical works are sparse; the rate of the microbially-induced urea hydrolysis has been evaluated (Fujita et al., 2008), but research on the prediction of evolutions in the mechanical and/or the hydraulic properties of the improved materials induced by the MICP is not apparent.

In this work, the urease enzyme is adopted instead of using bacteria such as *Sporosarcina pasteurii*, often used as a promoter for the hydrolysis of urea, which, as described above, causes Ca^{2+} and CO_3^{2-} to precipitate as $CaCO_3$ and form into the void spaces and/or the surfaces of grains. Utilizing the enzyme itself is more straightforward than using bacteria, because the cultivation and fixation of bacteria (i.e., biological treatment) do not need to be considered in this work. A grouting technique, in which chemically-precipitated calcite is adopted as the cementing material, may be recognized as the calcite in situ precipitation system (CIPS) (Kucharski et al., 1996; Ismail et al., 2002a,b). The CIPS may be similar to the method that is being presented in this work. However, the CIPS is a commercial product and the composition of its chemical solution is not apparent. In this work, the compositions of the adopted solutions are clearly addressed. After introducing the grouting reagents into the soil samples, the evolutions in the mechanical and the hydraulic properties are examined through unconfined compression tests and permeability tests, respectively. Moreover, changes in the hydraulic conductivity are predicted by an advection–diffusion simulation by considering the calcium carbonate precipitation, and the predictions are compared with the actual measurements.

2. Experiments

In order to examine the workability of the grout materials utilized in this work, test-tube experiments are conducted. Then, a suite of unconfined compression and permeability experiments is conducted for the calcium carbonate-precipitated sand under various initial and boundary conditions by changing the amount of reactants. The reactants used and the experiments conducted here are explained in detail.

2.1. Materials

Urease (Kishida Chemical Co., Ltd.,: 020-83242) is found in bacteria and in several plants, such as sword beans, and is used throughout the current work as an enzyme to hydrolyze urea. The resulting carbonate ions are applied to produce the calcium carbonate being precipitated. The companion to calcium carbonate (i.e., calcium ions) is supplied from the calcium chloride solution, which is freely soluble in water (i.e., the solubility is 82.8 g/100 mL of water at 20 °C). The expected reactions to obtain the calcium carbonate precipitation, enhanced by the effect of urease, are expressed as follows:

$$CO(NH_2)_2 + 2H_2O \rightarrow 2NH_4^+ + CO_3^{2-} \quad (1)$$

$$CaCl_2 \rightarrow Ca^{2+} + 2Cl^- \quad (2)$$

$$Ca^{2+} + CO_3^{2-} \rightarrow CaCO_3 \downarrow \quad (3)$$

where $CO(NH_2)_2$ represents urea. A schematic of the whole process listed above and the grouting mechanism expected are illustrated in Fig. 1.

2.2. Test-tube experiments

In this work, urease, urea, and calcium chloride are used as reagents contained in the grout. The rate and the magnitude of calcium carbonate precipitation should be controlled by the amounts of those materials. Thus, the effects of the grouting materials exerted on the calcium carbonate precipitation are examined by conducting two different sorts of test-tube experiments. A schematic of the test-tube experiments is shown in Fig. 2. During the experiments, the solutions in the test tubes are stirred regularly by a rotating table to ensure complete mixing.

The aim of one set of test-tube experiments is to examine the rate of urea hydrolysis that is bio-catalyzed by the urease. When urea is dissociated into ammonium and carbonate ions (Eq. (1)), the pH of the solutions should increase correspondingly to the production of ammonium

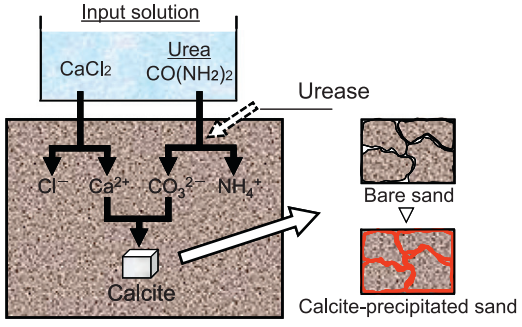

Fig. 1. Schematic of calcium carbonate-precipitation process and grouting mechanism.

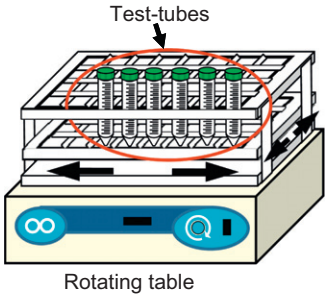

Fig. 2. Schematic of test-tube experiments.

Table 1
Experimental conditions of test-tube experiments.

Sample	Amount of urease [g/100 mL of solution]	Urea concentration [mol/L]	$CaCl_2$ concentration [mol/L]
TpH-1	0.5	0.5	0
TpH-2	1.0		
TpH-3	1.5		
TCa-1	1.0	0.5	0.5
TCa-2		1.0	1.0
TCa-3		1.5	1.5

ions. Therefore, the measurements of the evolution in pH with time may indirectly define the rates and the magnitude of the urea dissociation accelerated by the urease. Note that the rate of the changes in pH resulting from the production of ammonium ions is not equivalent to that of the calcium carbonate precipitation, and that the precipitation should take more time than the dissociation of urea. The experimental conditions for this purpose are listed in Table 1. As shown in the table, the concentration of urea solutions is fixed at 0.5 mol/L, while the amounts of urease are varied. The evolving pH is measured by a pH meter (KRK: KP-5F) at 0, 1, 2, 3, 6, 12, and 24 h after mixing.

The aim of the other set of test-tube experiments is to examine the calcium carbonate-precipitation characteristics depending on the concentrations of grout materials. The experimental conditions for this purpose are also listed in Table 1. As shown in the table, the amount of urease is fixed at 1 g/100 mL of water, while the concentrations of $CaCl_2$–urea solutions are varied. The solutions sampled 24 h after mixing were assayed by inductively-coupled plasma atomic emission spectrometry (ICP-AES) to quantify the Ca concentrations.

The results of the two different test-tube experiments are shown in Fig. 3. As is shown in Fig. 3(a), all measured pH levels increased rapidly at 1 h, and then approached a steady state after 6 h, although the case of TpH-1 showed a slight increase at 12 h. The peak pH for cases TpH-1, 2, and 3 ranged from 9.53 to 9.62, which shows no prominent difference among the experimental conditions adopted here. Fig. 3(b) represents the relation between the initial prescribed Ca concentrations and the consumed Ca

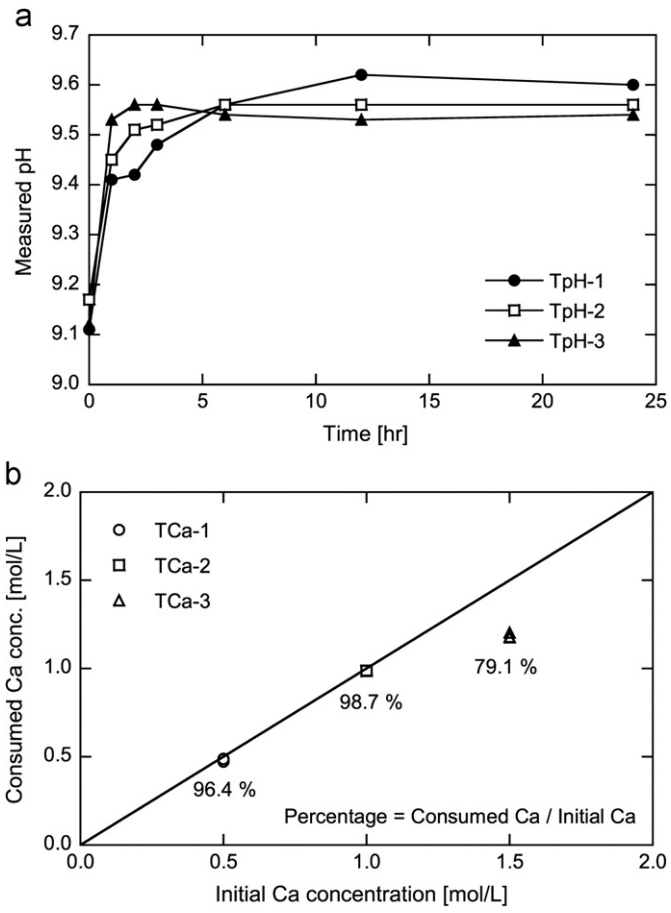

Fig. 3. Results of test-tube experiments ((a) changes in pH with time and (b) relation between initial Ca and consumed Ca concentrations).

concentrations that are equivalent to the initial values minus the measurements by ICP-AES. The average Ca consumption ratios to the initial values of TCa-1, 2, and 3 are 96.4, 98.7, and 79.1%, respectively. These results indicate that the high $CaCl_2$–urea concentrations relative to the amount of urease may restrain the activity of urease, which may in turn result in a reduction in the calcium carbonate precipitation.

The test-tube experiments have revealed both the rapid dissociation rates of urea, accelerated by the urease, and the importance of the relative concentrations between the urease and the $CaCl_2$–urea solutions.

2.3. Unconfined compression tests

In this section, unconfined compression tests are conducted to examine the effects of the improvement exerted on the stiffness and the strength of treated sand samples. The procedure to prepare the samples for the tests is as follows. The test apparatus is shown in Fig. 4. Firstly, 300 g of dry Toyoura sand, well-mixed with a certain amount of urease powder, is carefully pluviated in air to acquire a relative density of 50% (i.e., an initial porosity of 0.44) with sample dimensions of 50 mm in diameter and

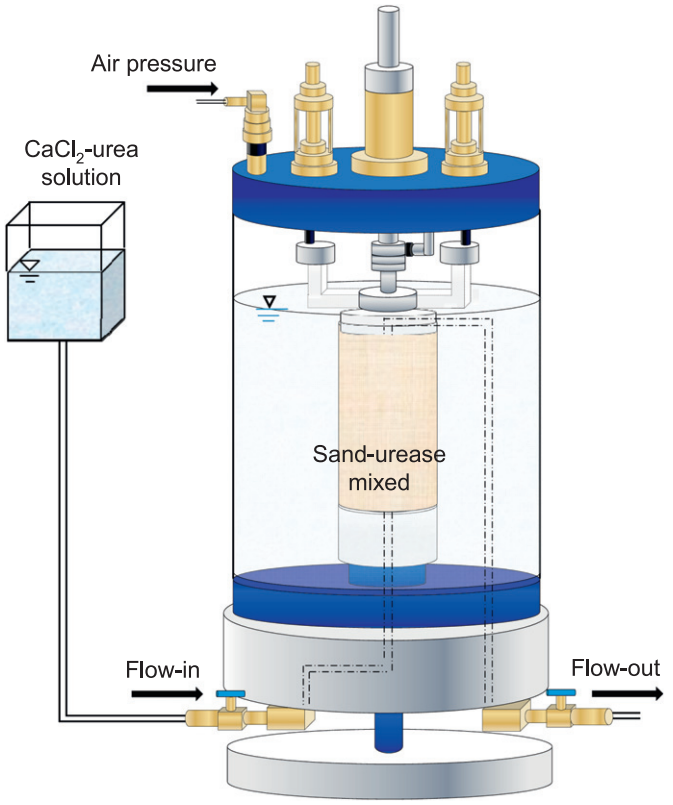

Fig. 4. Pressure cell for sample preparation.

100 mm in height (roughly 290 g of mixed sand is consumed in the sample preparation). The urease powder is pre-mixed with the sand in order to achieve homogeneous samples. Secondly, after the dry sample is evacuated to facilitate saturation, as the $CaCl_2$–urea solution is to be injected, a confining pressure of 50 kPa is applied. Thirdly, a concentration-fixed calcium chloride solution, blended with the same molar urea, is injected into the dry sand samples at the prescribed times, and then the samples are cured for 24 h within a pressure cell. Fourthly, 150 mL of distilled water is injected to flush out the byproducts of chloride and ammonium ions. Finally, the cured sand samples are taken out of the cell and are dried completely). The dried samples are used for the unconfined compression tests.

The test conditions for the unconfined compression tests are listed in Table 2. The concentrations of the $CaCl_2$–urea solution are 0.5 and 1.0 mol/L—the same molar concentrations for $CaCl_2$ and urea are blended, in advance. The amounts of urease, mixed well with 300 g of Toyoura sand, are 0.5 and 1.0 g. One hundred milliliters of the $CaCl_2$–urea solutions are injected into the samples (i.e., sand+urease) over approximately 0.5 h, and the same amount of solutions is injected 4 or 8 times at 2-h intervals. Here, a maximum amount of calcium carbonate (i.e., calcite) precipitation is estimated to be 40 g (i.e., 0.4 mol) for every test where the reactions in Eqs. (1)–(3) fully proceed. To check the reproducibility, two samples are made for each test condition.

Table 2
Experimental conditions for unconfined compression experiments.

Sample case	Sample name	Concentration [mol/L][a]	Injection number	Urease [g][b]
C1	bio-1, 4, 6	0.5	8	1.0
C2	bio-2, 5	1.0	4	1.0
C3	bio-3, 7	0.5	8	0.5

[a]Concentrations of $CaCl_2$–urea solutions.
[b]Urease is mixed with 300 g of the Toyoura sand.

Prior to the unconfined compression tests, the improved sand sample of bio-1 (Fig. 5), that is not used for the compression tests, was examined by an X-ray diffractometry (XRD: Rigaku RINT 2200) and a scanning electron microscopy (SEM: Hitachi S-2700 SEM). The sand sample was saw-cut and several specimens were prepared for both analyses. Fig. 6 shows representative XRD results for the bare sand and the improved sand samples. As is most clearly shown in Fig. 6(b), a distinct peak of calcite is observed in the improved sand, guaranteeing that calcite is the precipitated material within the pore spaces that have been induced by the solution injections. Fig. 7 shows the SEM results for the pre- and the post-improved samples. The precipitated materials are the size of a few tens of microns, and are situated on the free-surface and at the boundaries of the grains. These materials are most likely to be calcite, as is clear from the XRD results. The precipitated calcium carbonate, complicatedly stuck around the grains, should result in the manifestation and the augmentation of stiffness and strength.

Using the other improved sand samples of bio-2 to bio-7, unconfined compression tests have been conducted. Fig. 8 shows the observed relations between the normal strain and the normal stress, and the secant elastic modulus at 50% of the peak strength (E_{50}) and the unconfined compressive strength (UCS) are evaluated from the observation (Table 3). In Fig. 8, the early behavior does not show a nearly linear trend, but a positive curvature. This is likely to be attributed to a slight sliding along the grain boundaries and the compression of micro-pores, and should be typical behavior for rock materials (e.g., Jaeger et al., 2007). As is apparent, the observed ranges for E_{50} and UCS of $\sim$50 MPa to $\sim$160 MPa and $\sim$400 kPa to $\sim$1.6 MPa, respectively, are, roughly speaking, comparable to those of weak rocks. The results have revealed that this calcium carbonate precipitation method adequately solidifies loose sand. The bio-5 (or C2) results show the strongest values among all the conditions, while the bio-3 (or C3) results are the weakest. It is understood that the concentrations of the solutions injected and the amounts of urease enhancing the reaction are key parameters to controlling the stiffness and the strength of the improved samples.

Although a maximum precipitation of calcium carbonate is estimated at 40 g for all cases, the actual amounts of precipitated calcium carbonate need to be examined. For this purpose, after completing the compression tests, the

Fig. 5. Improved sand sample of bio-1.

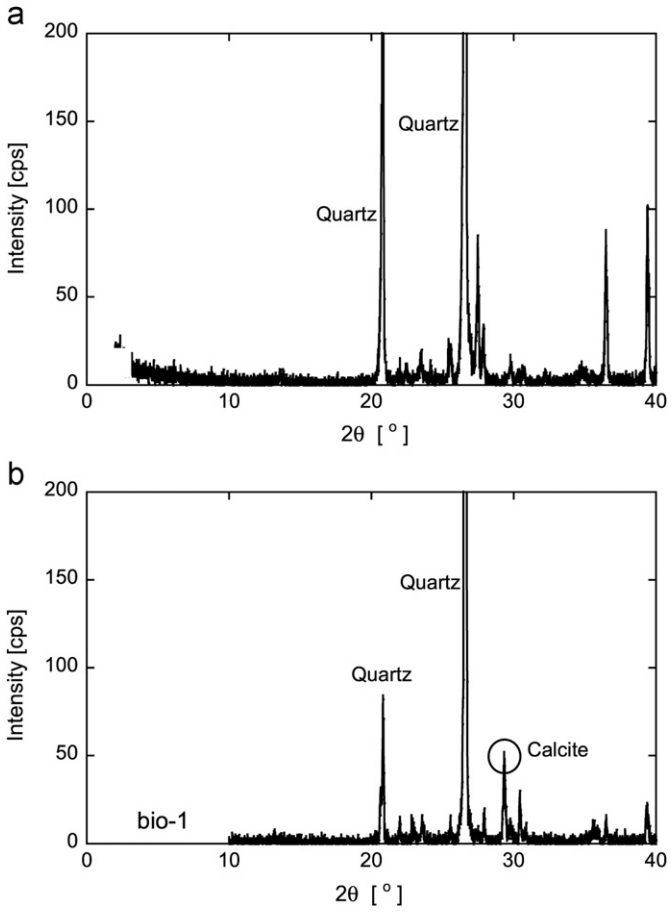

Fig. 6. XRD results of (a) bare sand and (b) improved sand (bio-1).

samples were rinsed using a 0.1 M HCl solution three times to dissolve the precipitated calcium carbonate. Then, the disaggregated samples were dried again, and the amounts of calcium carbonate were evaluated by comparing the weights of the pre- and the post-rinsed samples. A relation between the amount of calcium carbonate and *UCS* is depicted in Fig. 9. It is clear from the figure that the

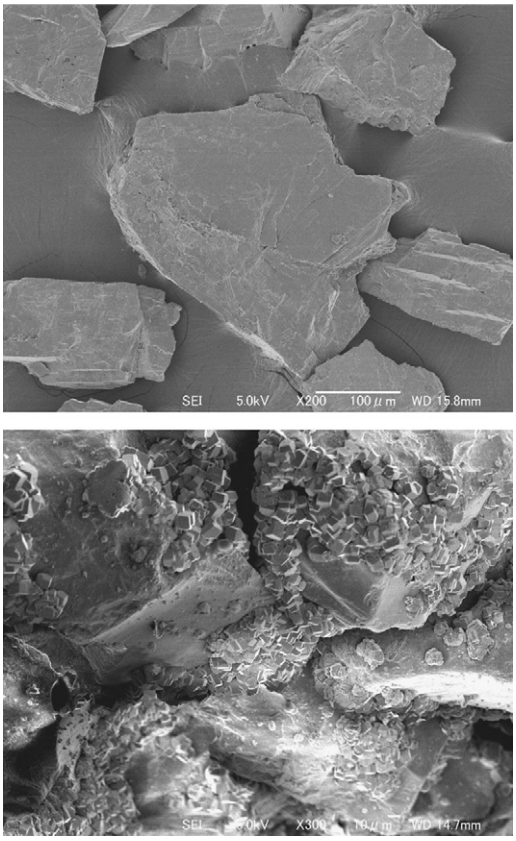

Fig. 7. SEM results of bare sand and improved sand (bio-1).

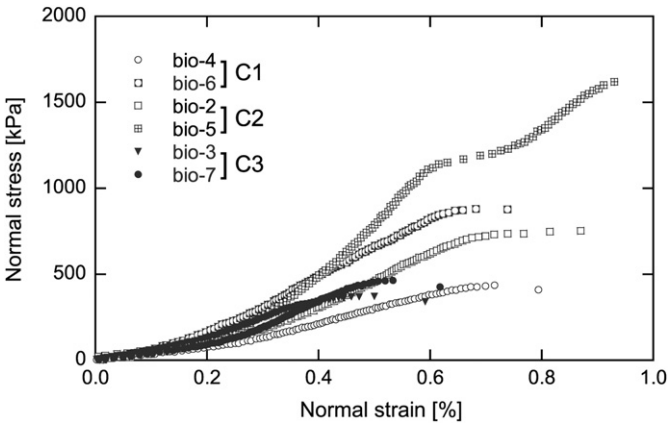

Fig. 8. Obtained results of relation between normal strain and normal stress.

actually-precipitated amounts range from 30 to 60 wt% against the maximum. Although some exceptions are observed, there is a tendency for more strength to be observed with a larger amount of calcium carbonate, which is reasonable. The broken lines in the figure represent 5 and 10% of the initial pore volume. Thus, the *UCS* of the improved sand may lie between 400 and 1600 kPa where 5–10% of the pore volume is occupied by precipitated calcium carbonate. In order to compare the results in this study with data from literature, a relation

Table 3
Evaluated E_{50} and *UCS* from unconfined compression experiments.

Sample case	Sample	ε_f [%][a]	E_{50} [MPa]	*UCS* [kPa]
C1	bio-4	0.706	53.5	435
	bio-6	0.676	120	890
C2	bio-2	0.870	84.1	754
	bio-5	0.918	160	1620
C3	bio-3	0.481	73.5	373
	bio-7	0.514	71.5	466

[a]Compressive strain at peak stress.

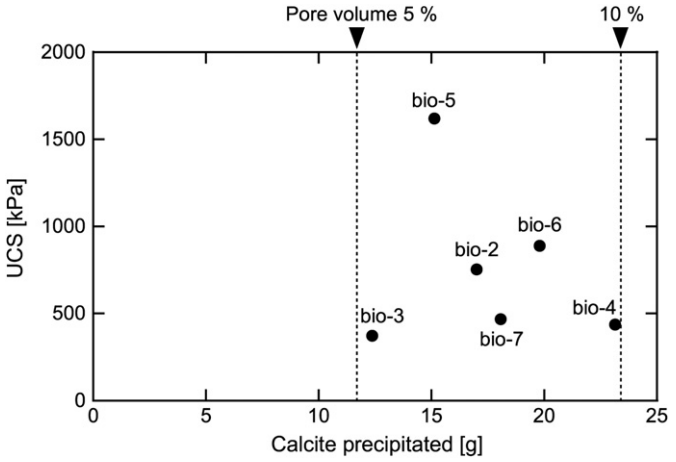

Fig. 9. Relation between precipitated calcium carbonate and *UCS*. Broken lines represent 5 and 10% of initial pore volume.

between the amount of calcium carbonate and *UCS*, which is evaluated using the results shown in van Paassen et al. (2010), is depicted in Fig. 10. Since the ratio of calcium carbonate to the weight of dry sand is shown for reference, the amounts are estimated by assuming that the weight of the sand sample is 300 g, which is equivalent to that used in this study. As shown in the figure, the results in this study may follow a regression curve evaluated from those by van Paassen et al. (2010), and may be compatible with those existing data. Taken together, the results of the unconfined compression tests indicate that the *UCS* of the sand improved by this injection method may be controlled when the amount of actual precipitation has been well predicted.

2.4. Permeability tests

In this section, permeability tests are conducted to examine the effects of improvement on the permeability of the treated sand samples. The procedure for the sample preparation for the permeability tests (Fig. 11) is similar in part to that for the unconfined compression tests explained above, but also different in part. It is the same in terms of the amount of Toyoura sand, urease, urea, calcium chloride, and the dimension of the samples. It is different in that the mixed sand is pluviated into an acrylic cylinder to acquire a relative density of 50%, and that the permeability tests are conducted at prescribed intervals after injecting the solutions. Note that no confining pressures are applied throughout the tests.

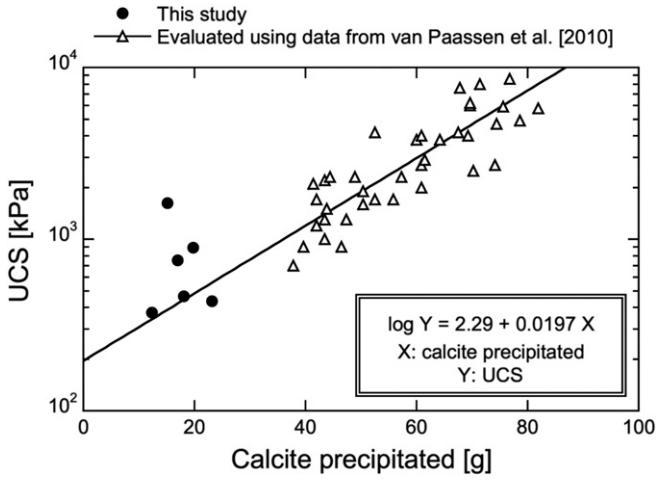

Fig. 10. Relation between precipitated calcium carbonate and *UCS*. Open triangles are evaluated using data from van Paassen et al. (2010) (S5).

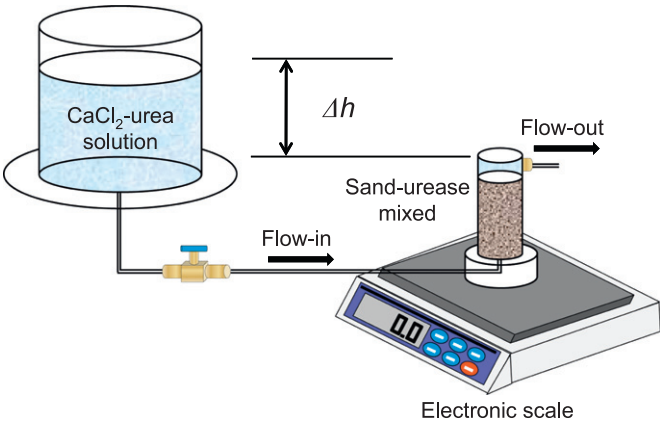

Fig. 11. Schematic of permeability tests.

Table 4
Experimental conditions for permeability experiments.

Sample case	Concentration [mol/L][a]	Injection number	Urease [g][b]	Maximum precipitation [g]
P1	0.5	1	1.0	7.5
P2	1.0	1	1.0	15.0
P3	0.5	1	2.0	7.5
P4	1.0	1	2.0	15.0
P5	0.5	4	1.0	30.0
P6	1.0	4	2.0	60.0

[a]Concentrations of $CaCl_2$–urea solutions.
[b]Urease is mixed with 300 g of the Toyoura sand.

The test conditions for the permeability tests are listed in Table 4. The concentrations of the $CaCl_2$–urea solution are 0.5 and 1.0 mol/L, which are equivalent to those of the unconfined compression tests. The amounts of urease are 1.0 and 2.0 g against 300 g of sand. One hundred and fifty milliliters of $CaCl_2$–urea solutions are injected into the samples over approximately 0.5 h, and the same amount of solutions is injected 1 or 4 times at 2-h intervals. After the completion of the final injection, the hydraulic conductivity is measured under a constant-head condition at 0, 1, 2, 3, 6, 12, and 24 h. In a series of tests, the six different conditions seen in Table 4 are adopted. The number of solution injections is just one for P1–P4, and four for P5 and P6.

The temporal changes in hydraulic conductivity, observed for P1–P4, are shown in Fig. 12(a). The initial hydraulic conductivity of ~0.04 cm/s decreases monotonically by 60–70% for all cases; it reaches a steady state within roughly 5 h. The monotonic decrease in hydraulic conductivity should be attributed to the calcium carbonate precipitation that occurs and gradually increases after the solution injection. The ultimate values for P1 to P4 are 0.019, 0.012, 0.011, and 0.010 cm/s, respectively. The results show that the molar concentrations of the injected solution (i.e., 0.5 or 1.0 mol/L) and the amount of urease (i.e., 1.0 or 2.0 g/300 g of sand) do not significantly influence the changes in permeability when the number of solution injections is just one.

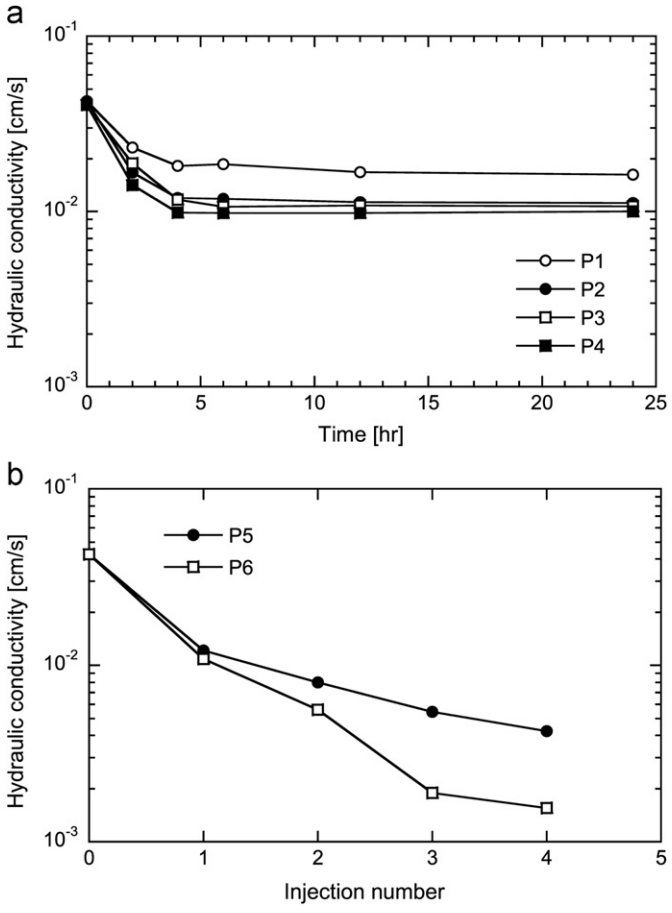

Fig. 12. Evolution of hydraulic conductivity ((a) temporal changes for P1 to P4 and (b) different injection numbers for P5 and P6).

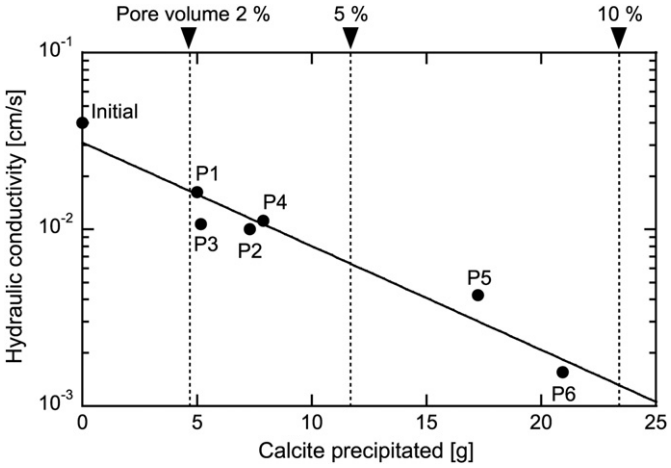

Fig. 13. Relation between precipitated calcium carbonate and hydraulic conductivity. Broken lines represent 2, 5 and 10% of initial pore volume.

In contrast, when the injection number is increased, the decrease in hydraulic conductivity 24 h after the injections is apparent (Fig. 12(b))—the more injection numbers, the more decreases are observed. The ultimate hydraulic conductivity (i.e., 4.2×10^{-3} and 1.5×10^{-3} cm/s for P5 and P6, respectively) decreases by roughly one order of magnitude after the fourth injection, as compared to the initial values. Moreover, the decrease under the higher concentration condition (P6) is greater than that under the lower condition (P5), which is reasonable because more precipitated calcium carbonate may clog more pore spaces within the sample. The decrease measured in the permeability tests is relatively significant (ca. one order of magnitude reduction), but is compatible to the decreases measured in the permeability tests conducted using the samples improved by the similar bio-grouting technique (Nemati and Voordouw, 2003; Kawasaki et al., 2006).

As examined in the previous section, the amount of actually precipitated calcium carbonate is also evaluated through the above-mentioned acid leaching. The relation between the precipitated calcium carbonate and the observed hydraulic conductivity is depicted in Fig. 13; it shows an obvious log-linear tendency between them. This indicates that the permeability of the sand improved by this injection method may be controlled when the amount of actual precipitation has been well predicted.

3. Model predictions

During injections of the grouting materials proposed in this work, an advective and dispersive transport of the solutions, together with chemical reactions of the calcite precipitation, occur within the pore spaces of the targeted soils. Thus, the process of the chemical reactions should be solved in a model that takes into account the advection–dispersion process. In this work, a suite of mathematical

equations, used for the transport simulations, is presented. Then, a comparison is made of the results between the measurements of the permeability tests and the predictions.

3.1. Mathematical formation for solution transport with chemical reactions

In this work, a non-isothermal reactive geochemical transport code, TOUGHREACT (Xu et al., 2004), is utilized to follow the evolution in permeability resulting from calcium carbonate precipitation mediated by enzyme-driven mineralization. Therefore, a whole calculation procedure is explained in detail by Xu et al. (2004). In this section, a summary of the calculation adopted in this work is explained.

Calcite precipitation is only considered for chemical reactions in this work. The governing equation is the advection–diffusion equation with chemical reactions, namely,

$$\frac{\partial(\phi C_j)}{\partial t} = -\nabla(uC_j) + \tau\phi D\nabla^2 C_j + R_n, \tag{4}$$

where ϕ [–] is the porosity and C_j [mol/m^3] is the concentration of aqueous chemical component *j*. u [m/s] is the Darcy velocity, τ [–] is the medium tortuosity, and D [m^2/s] is the diffusion coefficient. R_n [mol/m^3/s] is the reaction term (i.e., calcium carbonate precipitation), which is expressed as

$$R_n = -k_n A_n \rho_w \left|1-\boldsymbol{\Omega}_n^{\theta}\right|^{\eta}, \tag{5}$$

where k_n [mol/m^2/s] is the precipitation rate constant, A_n [m^2/kg] is the specific reactive surface area per kg H_2O, ρ_w [kg/m^3] is the water density, and Ω_n [–] is the kinetic mineral saturation ratio. Parameters θ and η are the constants that are constrained from the dissolution experiments. In this work, the measured BET specific surface area is adopted as A_n. For calcium carbonate precipitation, these parameters are considered unity. The rate constant is typically defined by

$$k_n = k_{25}\exp\left[\frac{-E_a}{R}\left(\frac{1}{T}-\frac{1}{298.15}\right)\right], \tag{6}$$

where k_{25} represents the rate constant at 25 °C, E_a [J/mol^1] is the activation energy, R [J/K/mol] is the gas constant, and T [K] is the absolute temperature.

The evolution of the porosity induced by the calcite precipitation is followed with time simply by evaluating the volume precipitated as

$$\phi(t+\Delta t) = (1 + R_n \times V_m \times \Delta t)\phi(t), \tag{7}$$

where Δt [s] is the time step in the calculations and V_m [m^3/mol] is the molar volume (i.e., 3.69×10^{-5} m^3/mol for calcite). The changes in permeability are calculated from the changes in porosity using the Carman–Kozeny relation (Bear, 1972), which ignores the changes in grain size, tortuosity, and the specific surface area, given by

$$K(t) = K_0\frac{(1-\phi_0)^2}{(1-\phi(t))^2}\left(\frac{\phi(t)}{\phi_0}\right)^3, \tag{8}$$

where K [m^2] is the permeability and subscript "0" represents the initial condition. Permeability may be converted to hydraulic conductivity, which is familiar to civil engineers and given by

$$k(t) = K(t)\frac{\rho_w g}{\mu}, \tag{9}$$

where k [m/s] is the hydraulic conductivity, g [m/s^2] is the gravity, and μ [Pa s] is the dynamic viscosity of the water. Specifically, an effective hydraulic conductivity in the vertical direction is evaluated to be compared with those obtained from the constant-head permeability tests, clearly defined as

$$\overline{k}_v(t) = \frac{h}{\sum(h_i/k_i(t))}, \tag{10}$$

where $\overline{k}_v(t)$ is the effective hydraulic conductivity in the vertical direction, h [m] is the sample height (i.e., 0.1 m), h_i [m] is the height of element i, and k_i [m/s] is the hydraulic conductivity of element i.

3.2. Comparison between measurements and predictions

To simulate the circumstances occurring in the permeability tests, such as the hydrolysis of urea by urease, a certain amount of carbonate and ammonium ions are made to exist in the calculation domain as initial conditions in the analysis. Then, 150 mL solutions of calcium and chloride ions, whose concentrations are equivalent to those used in the permeability tests, are injected into the domain, whose dimensions are equivalent to those of the test samples (i.e., 50 mm in diameter and 100 mm in height). Subsequently, a curing environment is simulated, after the solution injection, by flowing de-mineralized water at an extremely slow flow rate (i.e., $\sim10^{-30}$ kg/s), whose manipulation is adopted because calculations of the chemical reactions are not executed under no-flow conditions. The parameters (Xu et al., 2004; Barkouki et al., 2011), and the initial and boundary conditions used for the analysis, are listed in Tables 5 and 6, respectively.

A comparison of the results between the predictions and the test measurements for P1 and P5 is shown in Fig. 14. As seen in the figure, the predictions significantly overestimate the actual values. This may be attributed to the conversion equation from porosity to permeability (i.e., Eq. (8)). Permeability in porous media is strongly dependent upon the grain size (or the related pore size and its distribution), but it is not considered in this equation. Moreover, the precipitation occurring within the test samples may not be fully homogeneous. If a relatively large amount is precipitated locally, this may impede water flow, resulting in a significantly greater reduction in permeability than that predicted. Therefore, this analysis

is incapable of following the changes in grain or pore size and its distribution, which should occur in the process of calcite precipitation.

Alternatively, the changes in porosity are compared between the predictions and the actual measurements. The porosity of the post-test samples is evaluated by adopting the method explained in Section 2.4 (i.e., weighing the amount of precipitated calcium carbonate by means of an acid leaching). The results are compared in Fig. 15. As shown in the figure, the predictions match the measurements for P1 and P5 quantitatively well. Moreover, by observing Fig. 14(a) and Fig. 15(a), it should be noted that the predictions follow the experimental behavior quantitatively well—the predicted porosity monotonically decreases and reaches a steady state around 5 h, which is congruent with the evolution of the measured hydraulic conductivity. As one may imagine, the predicted reduction in porosity should be controlled by an adopted calcite precipitation rate constant. Two different values of k_{25} for calcite are obtained from the literature—6.46×10^{-7} mol/m^2/s from Xu et al. (2004) and 3.81×10^{-7} mol/m^2/s from Nilsson and Sternbeck (1999). These values are slightly greater than that shown in Table 5. The predictions using k_{25} of 3.81×10^{-7} mol/m^2/s are also shown in Fig. 15. As expected, the rate in the early period and the reduction in the magnitude of porosity are slightly greater than those obtained using the original value shown in Table 5, but are still compatible with the test results.

Fig. 16 represents the changes in the porosity distribution with time under the P1 conditions. Before the solution injection, the initial porosity of 0.44 is prescribed in the whole domain. Then, the porosity decreases gradually with time from the bottom, as the curing period proceeds. After 6 h of curing, no conspicuous difference (i.e., a further decrease in porosity) is observed. Ultimately, a slight discrepancy in the porosity is apparent between the top and the bottom elements—the porosities predicted at the top and the bottom are 0.438 and 0.425, respectively. After the permeability tests under the P1 conditions, the porosity was actually evaluated at the top, the middle, and the bottom of the sample. The obtained results at the top, the middle, and the bottom are 0.430, 0.432, and 0.432, respectively, which are qualitatively congruent with the predictions.

The porosity discrepancy between the top and the bottom is attributed to the slow flow rate prescribed in this work, which is 150 mL/30 min, while an initial pore

Table 5
Parameters used for numerical analysis.

Parameter	Value
Grain diameter, d	210 μm
Particle density, ρ_s	2.64 g/cm^3
Temperature, T	20 °C
Initial porosity, ϕ	0.44
Specific surface area, A_n	0.98 m^2/kg[a]
Initial hydraulic conductivity, K_0	4.4×10^{-2} cm/s
Precipitation rate constant, k_{25}	1.0×10^{-8} mol/m^2/s[b]
Activation energy, E_a	62.8 kJ/mol[a]

[a] A_n and E_a are obtained from Xu et al. (2004).
[b] k_{25} is obtained from Barkouki et al. (2011).

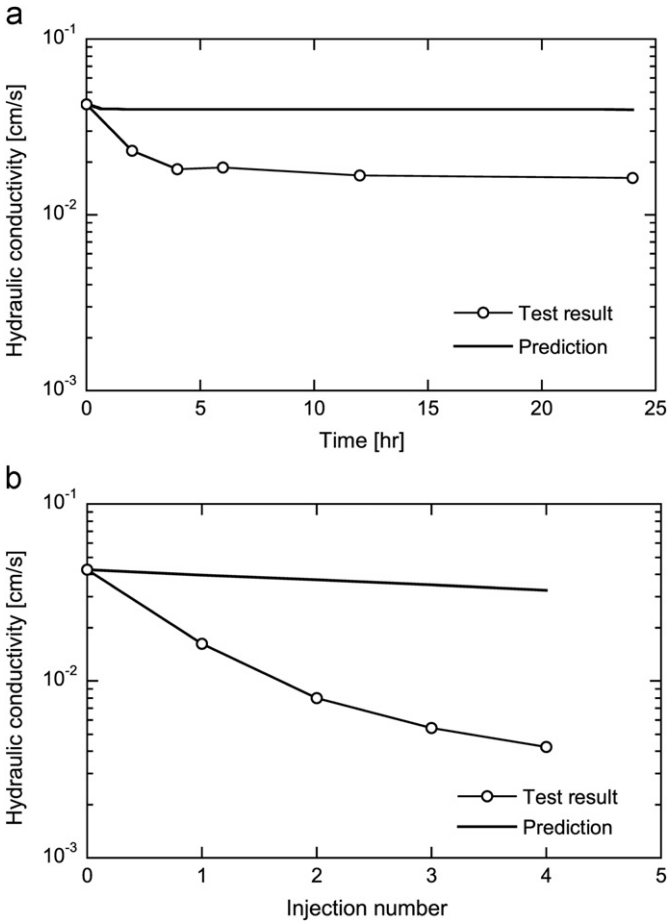

Fig. 14. Comparison of changes in hydraulic conductivity between test results and predictions for P1 and P5.

Table 6
Initial and boundary conditions for numerical analysis.

	Injection period (0–0.5 h)		Curing period (0.5–24 h)	
	Initial conditions	Boundary conditions	Initial conditions	Boundary conditions
Concentrations of Ca^{2+}, Cl^-, HCO_3^-, NH_4^+ [mol/L]	1.0×10^{-9}	0.50	< 0.50[a]	1.0×10^{-9}
Flow rate [kg/s]	–	8.33×10^{-5}	–	8.33×10^{-30}

[a] The remaining concentrations after consumed during the injection period are prescribed as the initial conditions.

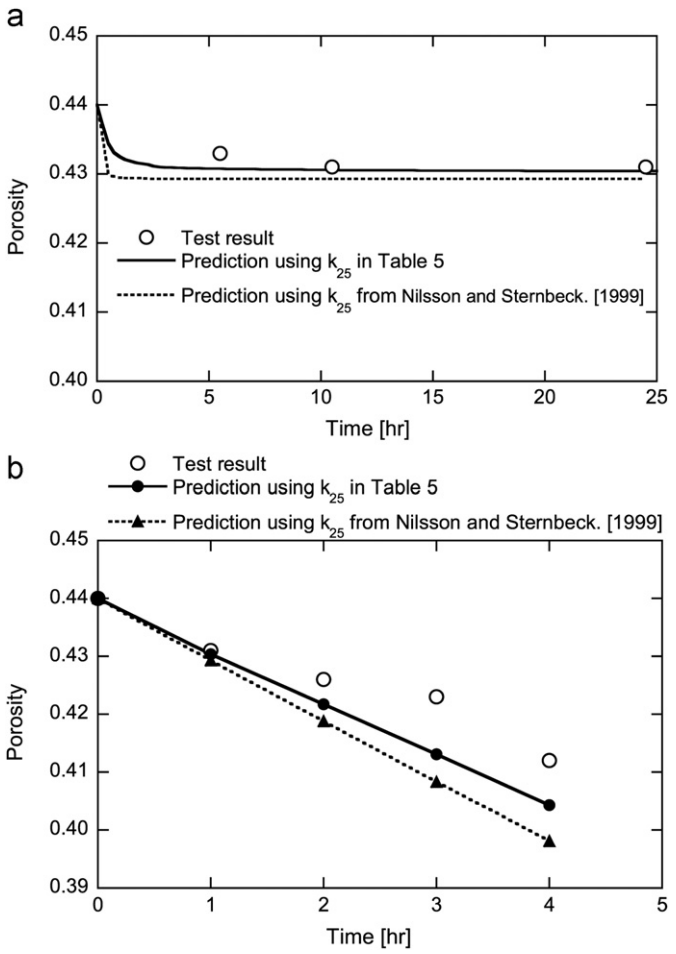

Fig. 15. Comparison of changes in porosity between test results and predictions for P1 and P5.

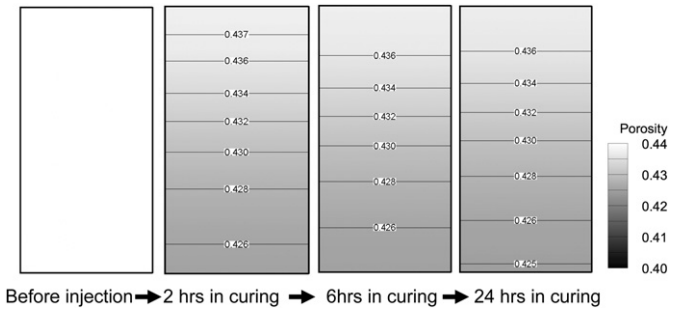

Fig. 16. Evolution of porosity distribution with time under P1 conditions.

volume of the soil sample is roughly 85 cm^3. Since the advection of the targeted ions of Ca^{2+} and CO_3^{2-} is slow, relative to the chemical reaction of the calcite precipitation, the targeted ions are consumed readily at the upper stream; and consequently, a discrepancy in porosity within the whole domain occurs. This result implies that a relative relation between advection (or related flow rates) and chemical reactions of the calcite precipitation should be fully examined and identified in advance whenever this grouting technique is to be applied at real sites.

The above outcomes lead to the conclusion that the numerical model should be effective for simulating the rate and the magnitude of the evolutions in porosity induced by calcite precipitation, and should be an important tool that supplements the grouting technique presented in this work. In order to achieve better predictions, proper relations between porosity and permeability, which take into account changes in grain size, tortuosity, and specific surface area, should be obtained.

4. Conclusions

This work has experimentally and numerically examined a grouting technique that utilizes calcium carbonate precipitation mediated by enzyme-driven mineralization. Unconfined compression and permeability tests, conducted for the improved samples, have shown the efficacy of the technique. Specifically, the stiffened samples are produced – unconfined compression strength ranges from 400 kPa to 1.6 MPa and the impervious properties are achieved – the permeability of the improved samples is reduced by more than one order of magnitude. Both the compression and the permeability test measurements implicate that the strength and the permeability of the improved body can be constrained when the amount of calcium carbonate being precipitated by this technique are well controlled, although further tests are needed.

Numerical analyses that simulate the advection–diffusion process, complemented by consideration of the chemical reactions of the calcite-precipitation kinetics, are conducted to replicate the changes in permeability measured in the permeability tests. The predictions significantly overestimate the actual measurements of permeability, but show a good agreement with the changes in porosity measured. This means that this model may be applicable to the prediction of the rates and the magnitudes of soil improvement resulting from the current grouting technique.

The grouting technique presented in this work, using the enzyme itself, may be more straightforward than that using bacteria which generates the enzyme of interest, because one can skip the process of cultivating the bacteria. The current grouting technique, in which the enzyme is mixed well within the soil samples prior to injecting the solutions, should be unsatisfactory. A solution containing the enzyme should be injected into the samples from the outside. This methodology will be examined and reported in the near future.

Acknowledgments

This work has been partly supported by research grants from the Institute for Fermentation, Osaka, Japan and the Shikoku Kensetsu Kousaikai. Their support is gratefully acknowledged. The authors also thank Mr. Tomohiro Sugimoto and Mr. Koichi Kado for their help with the experimental portion of this study.

References

Barkouki, T.H., Martinez, B.C., Mortensen, B.M., Weathers, T.S., De Jong, J.D., Ginn, T.R., Spycher, N.F., Smith, R.W., Fujita, Y., 2011. Forward and inverse bio-geochemical modeling of microbially induced calcite precipitation in half-meter column experiments. Transport in Porous Media.

Bear, J., 1972. Dynamics of Fluids in Porous Media. Dover Publications, Inc. (pp. 764).

DeJong, J.T., Fritzges, M.B., Nüsslein, K., 2006. Microbially induced cementation to control sand response to undrained shear. Journal of Geotechnical and Geoenvironmental Engineering, ASCE 132 (11), 1381–1392.

Foppen, J.W.A., Schijven, J.F., 2006. Evaluation of data from the literature on the transport and survival of *Escherichia coli* and thermotolerant coliforms in aquifers under saturated conditions. Water Research 40, 401–426.

Fujita, Y., Taylor, J.L., Gresham, T.L.T., Delwiche, M.E., Colwell, F.S., Mcling, T.L., Petzke, L.M., Smith, R.W., 2008. Stimulation of microbial urea hydrolysis in groundwater to enhance calcite precipitation. Environmental Science & Technology 42, 3025–3032.

Harkes, M.P., van Paassen, L.E., Booster, J.L., Whiffin, V.S., van Loosdrecht, M.C.M., 2010. Fixation and distribution of bacterial activity in sand to induce carbonate precipitation for ground reinforcement. Ecological Engineering 36, 112–117.

Ismail, M.A., Joer, H.A., Randolph, M.F., Meritt, A., 2002a. Cementation of porous materials using calcite. Geotechnique 52, 313–324.

Ismail, M.A., Joer, H.A., Sim, W.H., Randolph, M.F., 2002b. Effect of cement type on shear behavior of cemented calcareous soil. Journal of Geotechnical and Geoenvironmental Engineering 128, 520–529.

Jaeger, J.C., Cook, N.G.W., Zimmerman, R.W., 2007. Fundamentals of Rock Mechanics, 4th ed. Blackwell Publishing (pp. 475).

Kawasaki, S., Murao, A., Hiroyoshi, N., Tsunekawa, M., Kaneko, K., 2006. Fundamental study on novel gout cementing due to microbial metabolism. Journal of the Japan Society of Engineering Geology 47, 2–12.

Kucharski, E., Price, G., Li, H., Joer, H.A., 1996. Engineering properties of CIPS-cemented calcareous sand. In: Proceedings of the 30th International Geological Congress. Beijing, Brill Academic. pp. 92–97.

Le Metayer-Levrel, G., Castanier, S., Orial, G., Loubiere, J.F., Perthuisot, J.P., 1999. Applications of bacterial carbonatogenesis to the protection and regeneration of limestones in buildings and historic patrimony. Sedimentary Geology 126, 25–34.

Murphy, E.M., Ginn, T.R., 2000. Modeling microbial processes in porous media. Hydrogeology Journal 8, 142–158.

Nemati, M., Voordouw, G., 2003. Modification of porous media permeability, using calcium carbonate produced enzymatically in situ. Enzyme and Microbial Technology 33, 635–642.

Nemati, M., Greene, E.A., Voordouw, G., 2005. Permeability profile modification using bacterially formed calcium carbonate: comparison with enzymic option. Process Biochemistry 33, 925–933.

Nilsson, O., Sternbeck, J., 1999. A mechanistic model for calcite crystal growth using surface specification. Geochimica et Cosmochimica Acta 63, 217–225.

Stocks-Fischer, S., Galinat, J.K., Bang, S.S., 1999. Microbiological precipitation of $CaCO_3$. Soil Biology and Biochemistry 31, 1563–1571.

Sugimoto, D., Kuwano, R., 2008. Trial test on the evaluation of soil cementation generated by the function of microorganism. In: Proceedings of the 7th International Symposium on New Technologies for Urban Safety of Mega Cities in Asia. October 2008, USMCA, Beijing. pp. 669–674.

Van der Ruyt, M., van der Zon, W., 2009. Biological in situ reinforcement of sand in near-shore areas. Geotechnical Engineering 162, 81–83.

van Paassen, L.A., Ghose, R., van der Linden, T.J.M., van der Star, W.R.L., van Loosdrecht, M.C.M., 2010. Quantifying biomediated ground improvement by ureolysis: large-scale biogrout experiment. Journal of Geotechnical and Geoenvironmental Engineering 136, 1721–1728.

Whiffin, V.S., Van Paassen, L.A., Harkes, M.P., 2007. Microbial carbonate precipitation as a soil improvement technique. Geomicrobiology Journal 24 (5), 417–423.

Xu, T., Sonnenthal, E., Spycher, N., Pruess, K., 2004. TOUGHREACT User's Guide: A Simulation Program for Non-Isothermal Multiphase Reactive Geochemical Transport in Variably Saturated Geologic Media. Lawrence Berkeley Lab. Report LBNL-55460. Berkeley, California. pp. 192.